

HISTORY AND PRESENT STATE OF TRANSLATIONAL ELECTRO-OPTICAL APPLICATIONS TO MEDICINE

BRITTON CHANCE* and SHOKO NIOKA†

*Department of Biochemistry and Biophysics
University of Pennsylvania, PA USA*

*Britton Chance Center for Biomedical Photonics
Wuhan National Lab for Optoelectronics
Huazhong University of Science and Technology
Wuhan, China*

**Chance@mail.med.upenn.edu*

†*Nioka@mail.med.upenn.edu*

This paper reviews the history of the optoelectric devices applied to biomedical sciences in 20th century. It describes history of Vacuum tubes and Spectroscopies with the author's personal experiences, especially doublebeam spectroscopy. Further, the present developments of Near Infra Red (NIR) devices are described in translational biomedical applications. It includes particularly micro optoelectronics developments and present status of NIR breast cancer detection. Lastly, intrinsic molecular biomarkers are discussed especially NIR measurements of angiogenesis, hypermetabolism and heat production for cancer detection.

Keywords: History; vacuum tube; double beam spectrometer; NIR; Biomarker.

1. History of Vacuum Tubes and Spectroscopies

1.1. *The first electronics in optical devices; vacuum tube invention and improvements*

Before the discovery of the vacuum tube, the “string galvanometer” was the only device that recorded bioelectric signals without amplification. In 1904, J. A. Fleming (1849–1945) invented the vacuum tube in England making it possible to amplify the electrical signal and called it “valve”. In 1912, L. DeForest (1873–1961) invented the vacuum tube amplifier in the USA in order to cascade triodes to achieve high amplification and called it the “Audion”. With the vacuum amplifier, E. D. Adrian and Sir Charles Scott Sherrington,¹ the pioneers of electrophysiology, revolutionized neurobiology by studying neuronal signals. This vacuum tube made the measurements of very fast signals of neurons with high enough sensitivity and temporal resolution possible. Erlanger (1874–1965) and Gasser were awarded the 1944 Nobel Prize when they further developed electrophysiology by developing the most elaborate vacuum tube known as cascaded DC amplifiers. However, these developments

had poor stability and leakage characteristics, since the tubes [valves] were not properly evacuated, and had high grid currents. Later, RCA's development of the "Out Gassing capsule" greatly reduced the currents.

Much later, Dubridge invented "low leakage current" by using "suppressor grid input" which led to commercialization by Arnold Beckman (1900–2004)² in the mid 1930s. He and coworkers were able to exploit, without reference, vacuum tube amplifiers (so called high vacuum or hard tubes) that were suitable for the high resistance glass electrodes and the phototube.

In the 1930's, electrophysiologists working with engineers, notably J. P. Hervey and D. W. Bronk, were able to improve the Blumlein long tailed pair differential amplifiers³ with vacuum tubes using "Common Mode" rejection. At the same time, the Weston photovoltaic cell was replaced by the much more sensitive Vacuum Cs oxide on Silver [CsAg] photo cathode for red light and was supplemented by the blue sensitive Cs Sb cathode by Glover of RCA. Next, Jan Rajchman⁴ invented the photomultiplier (PMT) and called it "the multidynode Electronmultiplier squirrel cage phototube". (footnote; This became the standard of random noise generator for WW2 radio jamming).

At the same time as the concept of the moving coil galvanometer with photoelectric pickoff was replaced by the vacuum tube amplifier, the vacuum tube amplifier and the phototube were being modified to detect the motion of the electro physiologists galvanometer and to detect the motion of ships with respect to their magnetic compass by serving as auto-steering gear.⁵ The magnetic compass of history was necessary for the success of small and large ocean going vessels. After tedious 4 hour "watches" of staring at the dimly lit compass card in Chance's early teens, it occurred to Britton Chance that the mirror galvo pickoff, together with a self seeking photocell assembly and a servo system for following a compass directed light beam and a powerful servo motor would steer ships, small and large. Chance further developed the theory of servo-mechanisms to solve the problem of steering very large ships. Minorsky (1885–1970) and H. Hazen's⁶ theory of servo stability had been beneficial, the inertia of small and large ships and the low control ratio of the underpowered rudder created a difficult stability problem. The tests on small and large yachts empirically solved the stability problem by an adjustment of the "control ratio" and tests on a "small" Sun Oil Company tanker led to installation on the companies newest and largest tanker where Thyatron tube⁷ control of the servo motor was designed and tested—one of the first commercial uses of photoelectric thyatron servo control in the pre-world-War-II era.

1.2. The photoelectric spectrophotometer in 20th century

Based on Sir Isaac Newton's discovery of the light spectrum and his (erroneous) particle theory of light in the 18th century, in 1821, Fraunhofer reported on his first efforts to use a diffraction grating (rather than a prism). This enabled, Kirchhoff,

a chemist, to discover the relationship between emission and absorption spectra of matter in 1859. In 1913, Niels Bohr explained spectrum lines as electrons resulting from stable orbits which he called “stationary states” in higher-energy stationary state to a lower-energy one. In those times, Hand spectrometers (MacMunn’s visual spectroscopy) had been used. Keilin’s¹¹ studies of body pigments used the hand spectroscope to discover the cytochromes. Genn Millikan³⁹ used a photoelectric colorimeter, greatly improved for Chance’s study of the enzyme substrate compounds. Hartridge and Roughton studied oxy and deoxyhemoglobin kinetics using the Hand spectrometer. German chemists advanced the field by using the quartz monochromator spectrometer.⁸ Otto Warburg introduced precision spectroscopy and photochemistry to Biology and the study of the UV region of molecules, including the purified NADH and Flavin⁹ Nobel prize winning work supporting Keilin’s discovery of cellular oxidation and reduction. A. O. Beckman’s² work as a chemist, enabled him to combine visible light and cover the UV region with Carey’s quartz monochromator. Without Rajchman’s photomultiplier, Beckman used the “Dubridge electrometer” circuit in an enclosed “drierite” cabinet. Carey developed the quartz prism monochromator to open visible and ultraviolet regions. R. W. Woods designed a unique plastic replica grating for the elegant Coleman spectrophotometer. These inventions along with the Coleman double monochromator for the visible and near UV regions provided enough light for the CsSb photocathode to respond with a bandwidth of 10 or more HZ. This allowed post-war studies of many enzyme-substrates compounds in the laboratories of Theorell, Keilin and Chance. The new spectrometer was able to cope with the absorbance changes in the iron porphyrin spectra [Soret region] of the very dilute [less than 1 micromolar] heme iron enzymes and was used for a fast kinetic study of enzyme substrate compounds as obtained by the novel stopped flow method.^{10,12} Scientists were able to use the ratiometric devices to take advantage of the logarithmic relation of dynode voltage and the output signal of Ranchman’s squirrel cage dynode structure of the electron photomultiplier.⁴ This provided the absorbance outputs of spectrophotometers. The mercury arc lamp with its abundance of bright lines in the visible region, [especially in the 1 KW water cooled version] remains, in many cases, the light source of choice for fluorescence excitation of biological fluorochromes. The Beckman spectrometer dominated the field for the next few decades with a device that rivaled Charlie Chaplin’s caricature of the frustrated technician since using the machine took time and effort of many steps. In 1950s, C. C. Yang and Lennart Akerman’s contemporary inventions provided scientists with the self balancing automatic recording spectrophotometer.

As the essentiality of biological structure to biological function was recognized, the development of high resolution electron microscopy by Albert Claude,¹³ George Pallade, and Slater and Cleland attempted to apply the single beam spectrophotometer to the spectroscopy of turbid suspensions of a TCA extracted heart muscle with little success. Beckman’s “DU” spectrophotometers worked well with

transparent chemical solutions, but did not work well with biological materials and required novel optics, in spite of the Cardiod condenser, which paved the way for better light gathering, since biological materials scatter light.

Concurrently, Chance created the double beam spectrophotometer with two innovations that solved the problem of studies of living tissues and isolated mitochondrial spectroscopic study of biomaterials.¹⁴ The double beam spectrophotometer has the following features: (1) gather the scatter light as in the integrating sphere, (2) use a nearby reference wavelength, thereby minimizing the scattering distortion of a true absorption band. Since the MIE scattering law varies as the power of the wavelength, an isosbestic point that is nearby to the chosen absorption band of a biochemical reaction that causes the absorption band to substantially disappear. These features enabled Chance to construct the first spectrophotometer that rapidly timeshared a measure and referenced a wavelength from two monochrometers, implying upon a turbid material — a suspension of extracted mitochondria, microsomes or an intact organ heart, liver, or brain — and illumined a large area close-up detector accepting a large solid angle. This “dual wavelength” spectrometer is still a commercially used instrument. It also led to the discovery of new members of Keilin’s respiratory chain,^{15–21} of novel sets of enzymes in the microsomal fraction that revolutionized concepts of drug metabolism in the Estabrook Laboratory and enabled Glenn Millikan to realize his dream of a spectroscopic readout of the biochemical function of blood and cytochromes in living tissue.

The discovery that the two members of the Keilin’s respiratory chain, NADH and Flavoprotein, were fluorescent opened up a new field of Fluorescence microscopy of cells with one and two photon technology and provided the only intrinsic metabolism biomarker and gene expression in cell and molecular biology. This sparked the development of molecular beacons which mimic intrinsic beacons and lead to the field of molecular beacons and photo dynamic therapy, restricted to cell and tissue surfaces.

Subsurface signals of oxygen delivery and vascularity stimulated a reconsideration of the limitations of subsurface signaling with visible light. Therefore, in 1977, several investigators, particularly Kramer and Jobsis²² noted the advantages of minimized scattering and greater depth penetration of NIR wavelengths. With the NIR region, Chance *et al.* showed the skull actually gave an increase in the optical path length in the cat brain model²³ using time domain spectroscopy and using pico second NIR laser light. Shortly thereafter, Patterson²⁴ and Yodh²⁵ demonstrated that scattering and absorption factors could be calculated from the time and phase resolved spectroscopy, In collaboration with Delpy,²⁶ Gratton²⁷ and Lakowicz, the NIR field has provided the impetus for translational developments to study the muscle, breast, and brain in great detail with quantitative metrics of medical and scientific problems, exercise, cancer, stroke, and many others in parallel with MRI and PET.

2. The Present Developments of Near Infra Red (NIR) Devices in Translational Biomedical Sciences

The initial concept of massive optics and electronics have been deployed by relatively large size devices like the NIR brain imagers^{28–30} and breast cancer detection devices.^{31–33} However, the simplicity and power economy of the LED, the sensitivity of the Silicon Diode and the current state of Integrated Circuit manufacture at the CMOS level have enabled scientists and researchers to advance micro optical electronics and open a new field of medical devices. Both economical and pocket-sized devices that incorporate cellular phone technology of data storage and display predict a revolution in home care and rapid clinical diagnostics. This creates novel opportunities for communication and interaction between individual patients and medical experts. Optical technologies that use biomarkers may change the face of medical practice in many disciplines as the proposals are validated and statistics demonstrate the use of optics in diagnosis and disease management.

2.1. *Micro optoelectronics developments*

Biomedical translational applications require portability and wearability and emerging intravascular and endoscopy applications that will alter electro optic design principles.

The first of these applications grew out of the demonstration that NIR signals were of value in the non-invasive readouts of skeletal muscle function in normal and genetically deficient skeletal muscle. The search for an attachable and wearable devices emerged at the University of Pennsylvania laboratory and with the availability of the NIR LED and the silicon diodes. The circuit skills of MS Ma Zhou³⁴ and the design skills of Omron^{35,36} made it possible to attach a wearable muscle exercise monitor.

This first Photon migration device was followed by the finger transmission of red light modulated by the arterial pulse, affording the design of the pulse oximeter,³⁷ a vast improvement over Glenn Millikan and John Pappenheimer's ear oximeter of World War II.³⁸ The discovery that long division arithmetic gives detectable forebrain signals that differ from the arterial pulse signal initiated many studies of NIR signals from the human brain, in the occipital region initially claimed by Gabrielle Graton³⁹ to give a phase shift, using his brother's 100 megahertz G Weber type of fluorometer designs, a signal that is still controversial today. The main Biomarker of NIR today is the more solidly based absorption signals of blood volume and blood oxygen that are related to Ogawas's MRI "BOLD" signal.⁴⁰

The development of the wearable NIR detector was further advanced by a wearable detector of prefrontal cortex detection using 4 LED sources and 16 Silicon diode detectors. With this imager, the effects of learning and emotional responses in high school students over 7 years, consolidated the existence of the optical signals and verified that the optical patterns are highly individualized and may reflect the ethnic, training and the native ability of the multiracial population of the inner city

school children of Philadelphia.^{41,42} Other applications of the Runman principle emerged, especially the study of brain hemorrhage by Infrascan.⁴³

As the discomfort and low scores of X-Ray mammography became well published, the experience of close phobia and deafening sound of the gradient coils of MRI became known, there emerged a major health care cost. Therefore, the University of Pennsylvania laboratory undertook a test to use the Run Man principle to detect blood volume increments and deoxygenation biomarkers of early breast cancer. The first studies were in Wuhan. Later, a multi wavelength and multidetector array, studies were conducted at HUP. After 7 years of data accumulation, statistics were obtained that were acceptable to the Radiologic community and spurred NIH into a very large round of funding⁴⁴ for NIR breast cancer detection but none of the grantees have provided an acceptable solution to reach underserved high risk young patients. Therefore, we will address a new concept of an accessible and wearable self scannable device.

3. Present Status of NIR Breast Cancer Detection

3.1. *Cancer detection devices*

To date all Breast cancer detection devices are “wired” with multiple sources and detectors covering both fixed breasts with fiber optics or CCD coupling and computational demands for a subsequent localization and thus are not suitable for frequent studies required for early cancer detection by the high risk subjects. With the impetus provided by cell phone technologies, the consideration of a new generation of medical technologies that both acquire and display important medical information required for diagnosis and referrals. To this end we show the design and performance data on time multiplex and frequency domain self-scan detectors/localizers of human breast cancer from the instrumentation point of view. The detection of early breast cancer has been successfully achieved by attached and hardwired breast cancer detectors⁴⁴ and by larger devices.^{31–33}

General System Design and System Features A Personal Self Care breast cancer detector must have three key features, (1) It must localize the suspicious subsurface object, (2) It must acquire Biomarker signals of high Sensitivity/Specificity, and (3) It must store and display the current data and compare to all previous data. The Concept of the device is that a Handheld battery operated device with NIR multiwavelength sources and miniature detectors coupled to modulation and demodulation circuitry that indicates the detection of a suspicious subsurface object localizing three Biomarkers of cancer. This has either Dual source/single equidistant detector or Dual detector/equidistant single source system. The two systems are as follows:

Phase Modulation The group of systems termed “Phased Array” have the great advantage of background cancellation in this case by two antiphase sources and a single detector that gives a null signal with no suspicious object present and a

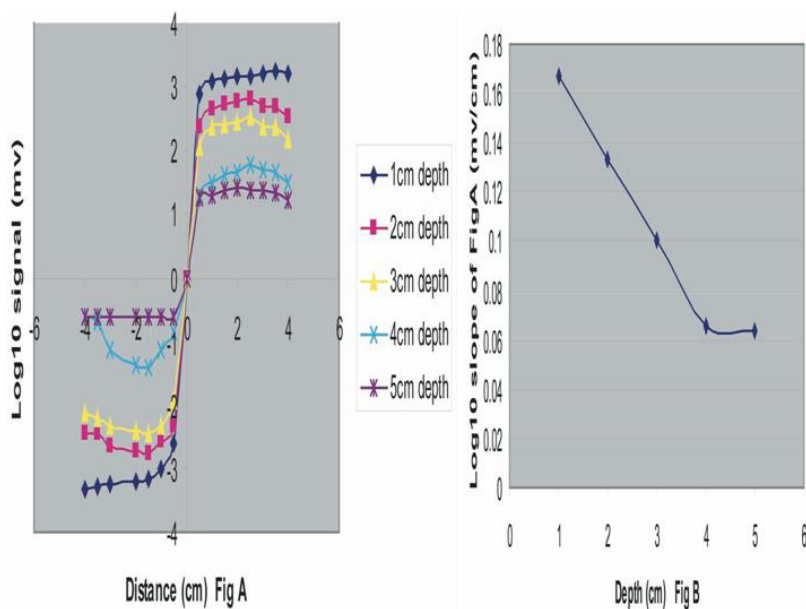


Fig. 1. The results of manual scanning of the handheld device (circuit design of Fig. 2) across a 1 cm^3 phantom at depths of 1 to 5 cm in a blood-lipid model mimicking the human breast. Negative signals (left side of diagram) will give a green light and positive signals a red light (right side of the diagram), with a transition zone of less than 6 mm.

phased signal depending upon the location of the object with respect to the its “Antiphased Array”.⁴⁵ Signal amplitudes are obtained by switching the from Anti-phase to In-phase at the closest approach to the subsurface object (see below under Localization signal). Frequency encoding can be used for multiwavelength sources.

Localization Signal for Phase Modulation As the Scanner is moved over the breast, as a suspicious subsurface object is approached, the nearer optical pattern will be attenuated and the phase null becomes unbalanced causing a green LED indicator to be illuminated. The unbalanced signal will increase as the object is approached and, with further movement, will decrease as the second anti-phase optical pattern is approached, falling to zero as the subsurface cancer is localized and reverse sign as it is passed, illuminating a red LED. The maximum signals are obtained at the null when the object is equidistant from the two anti-phased sources and are summed at that point by a switch to the in-phase connection (see below).

The circuit design takes advantage of the phased array, dual LED developments of Knuttel, Yu, Chen and ourselves^{46,47} for accurate tumor localization at the phase null position. Thus, the novel concept here is the combination of an anti-phase phase localizer together an in-phase signal detector, with direct localization indication to minimize readout time and to maximize the tumor search effectiveness. It is possible

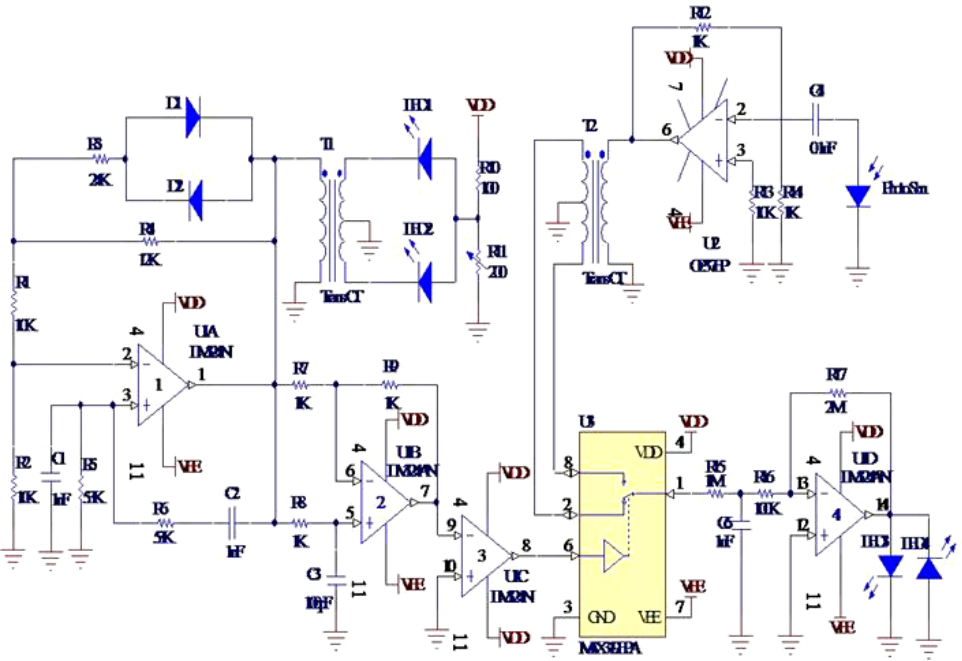


Fig. 2. Phase Modulation Home Care Scanner circuit for a single wavelength breast cancer detector.

to use time multiplex for the additional wavelengths in the Phase Modulated system instead of frequency encoding for multi wavelength operation.

The circuit components of Fig. 2 include 4 IC, 2 transformers, 1 switch, 4 LEDs. The system operates at a frequency of 3 KHz and drives LED 1 and LED 2 (both 805 nm) in anti-phase through the split secondary of Pico transformer T1 at a power level of about 5 mW. A 3 KHz oscillator with transformer coupled anti-phase LEDs at 805 nm with suitable bias is provided to modulate the LEDs linearly at the usable range of 20 to 50 mA. Here, miniature center tapped audio transformers are used to provide anti-phase drive (PICO transformer). The Wein Bridge audio oscillator driven LED signals are picked up by the 4 × 4 mm silicon diode (Hamamatsu) and amplified by a current-to-voltage converter which in turn drives a second mini-transformer. The center tapped secondary signals are sampled by the bi-directional switch detector which affords common mode rejection and differential sensitivity to the signal from the detectors. In this case, visible indication of localization is indicated by red and green LEDs which tell the operator when a signal has been detected and to move the detectors to equalize the signal intensities where the green LED signal changes to red and vice versa with a sensitivity for a positional change. Reversal of the polarity of the AC drive for one of the two LEDs is required in order to convert the two LED outputs to the same phase so that the switch detector will add the signals rather than subtract them. Thus, a double throw

double pole electronic switch, activated by a spring loaded push button on the Handheld device is operated in order to record the signal magnitudes, the in-phase signals are digitized and stored in an 8 bit memory with date, time, operator ID, etc.

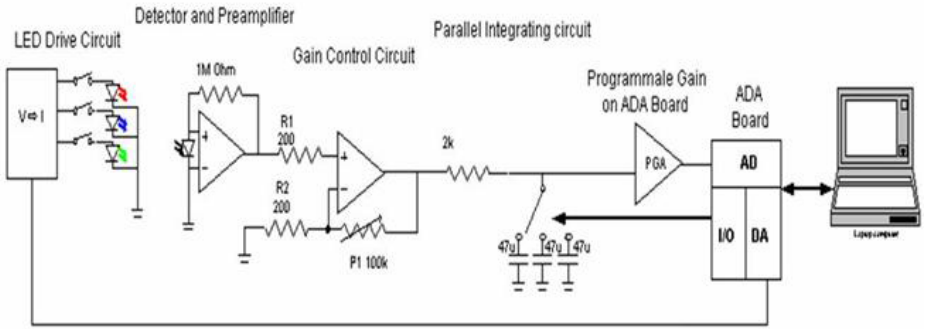
Time Modulated System Similarly, the two possibilities for source and detector combinations are available, but in this case the two sources are time multiplexed at, for example, 10 msec with a switched detector of the detector outputs which are subtracted for localization signals. As the manual scan proceeds, the display will indicate a null output for no subsurface object and a positive or negative signal if a suspicious object is present. The signals are added for the 3 Biomarker Magnitudes. Multiwavelength sources are accommodated by time multiplex (TMS) and multiplex switch detection. One of the TMS systems⁴⁴ has a single source and 8 detectors and the processed signals from two opposite detectors are subtracted. The process is repeated for the orthogonal pair of detectors creating two orthogonal vectors as sides of a right triangle, which is a vector pointing in the direction of the subsurface cancer, and the magnitude of which increases to a maximum as the cancer is approached. The localization vector decreases to a low level when the light source is directly over the subsurface cancer, and reverses direction as the scan is continued. The 8 detector signals are recorded at the vector minimum. The subjects may scan their breast at 1 cm/sec so that a 1 cm cancer would be well accommodated by a 2 Hz bandwidth for the localization signal and 3 sec averaging time for the 8 signal magnitudes.

An elaboration of the TMS system of Fig. 3 will incorporate the following — A digital clock for 5–10 ms sequential pulses for the 5 LEDs. Two equidistant Silicon Diode detectors (3 to 5 cm) coupled to digitally controlled current to voltage amplifiers followed by 2 sets of 5 channel time switches and 1 sec RC filters coupled to ADC. DSP and signal subtraction for dual wavelength signals and digital display of the two sets of 3 Biomarkers in the 3D monogram. Localization signals obtained by subtraction of the two orthogonal sets of 3 Biomarkers for localization signals and activation of the vector localization indicator.

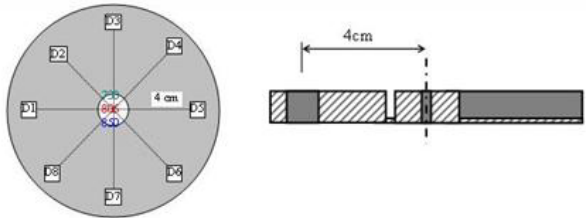
3.2. Biomarkers of NIR signals

Interest in the several Biomarkers of cancer has stimulated recent resurgence of multichannel systems with frequency, time and phase encoding. In fact, the study of the NIR region has revealed 3 Biomarkers of Blood volume, deoxygenation, and heat which require dual wavelength NIR spectrophotometry, 10 narrow band signal channels. For heat measurement, the addition of more wavelengths is necessary to increase diagnostic capability. The addition of the two dual wavelength channels at 760,850, for deoxyhemoglobin measurement and 970 and 920 nm for metabolic thermogenesis measurement to both of the above systems. This is made possible in the case of the phase modulation system simply by adding 4 more circuit boards each encoded at different audio frequency, 300, 900, 1200, and 3600 Hz, and for the

The diagram of control box:



The illustration of probe:



730nm, 805nm, 850nm: three wavelengths of LED light source; D1, D2, ... D8: eight detectors of the probe

Fig. 3. A 3 wavelength time multiplex system (TMS) with sample and hold detection. A source and equidistant 8 detectors are mounted in the periphery of the probe.

time multiplex system 4 additional 10 msec light pulses, multiplex switches, detectors and filters.

Thermogenesis Biomarker. As the Fig. 4 shows, Barlow finds the absorption band of water at 970 nm is temperature sensitive and is very useful signal to detect the greater metabolic activity of the growing cancer relative to the non-growing normal adult tissue. These signals are clearly shown in the following work of Barlow⁴⁸ and of Estabrook and Poe⁴⁹ in Figs. 4 and 5.

On the left of Fig. 4 are the hemoglobin signals overlapping the water a signal and on the right are a series of difference spectra of 1 mm thick water as the temperature is both decreased and increased with respect of 37 degrees identifying 760 and 850 as suitable for dual wavelength measurement of hemoglobin deoxygenation and 970 and 928 nm as suitable for dual wavelength measurement of tissue temperature with a sensitivity of 0.010 optical density per degree C. Baseline 37 degrees with lowering, showing that 968 nm is an appropriate measuring wavelength and 920 nm is a suitable reference wavelength. A signal increment of 0.010 optical densities per degree for a 1 cm optical path is calculated. In the case of measurement of deoxy-hemoglobin at 760 nm, a reference wavelength of 850 nm is suitable, and in the case of thermogenesis at 970 nm, the nearby reference wavelength of 920 nm is suitable.

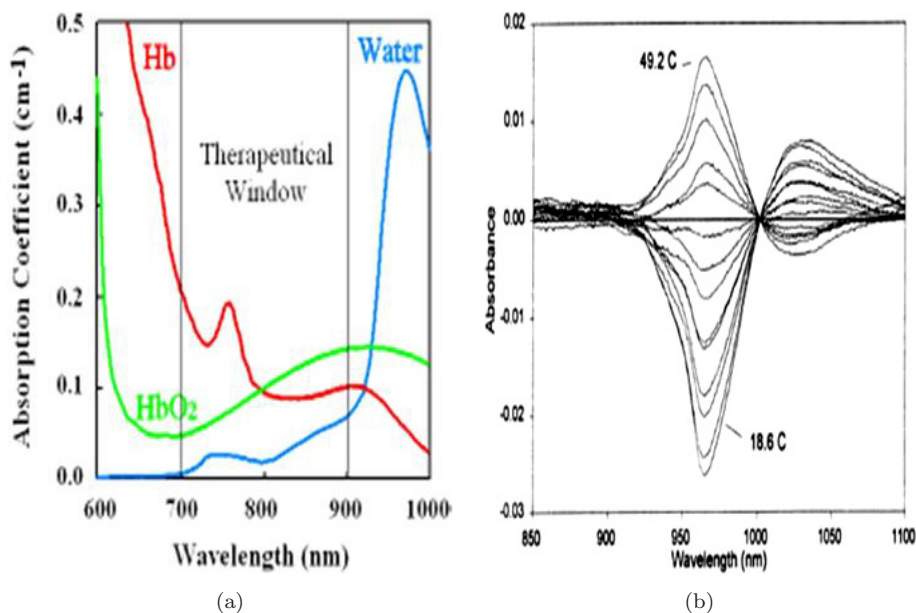


Fig. 4. (a) Merging of the hemoglobin and water absorption spectra to an arbitrary scale to show their spectral overlap and the optimal “windows” for minimal crosstalk of the three metrics to be studied. (b) Sensitivity of water absorption spectrum to temperature. Thermal difference spectra of water in a 1 mm pathlength (Kelly *et al.*, 1995).

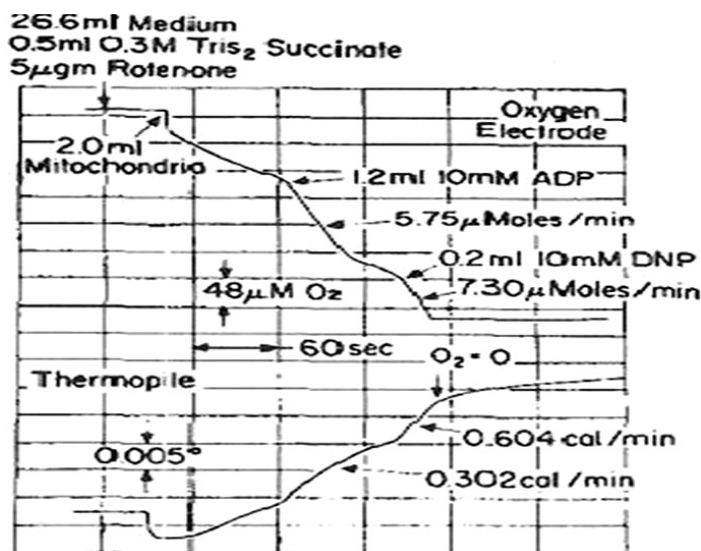


Fig. 5. Mitochondrial Thermogenesis. Estabrook and Poe's calorimetric data on mitochondrial heat generation in activation by phosphorylation of ADP to ATP and further heat generation in the DNP uncoupled state (Poe and Estabrook, 1967).

In both anti-phase and time multiplex circuits, the reference signal is subtracted from the measure signal.

Detection of Mitochondria Thermogenesis In order to demonstrate that the metabolic activity of the cancer mitochondria can be measured by NIR absorption and by thermogenesis, the reprint of Fig. 5 displays the data of Estabrook and Poe using differential calorimetry that compares lowering of oxygen in water with the heat produced in this reaction under conditions of ADP phosphorylation to ATP and the uncoupled state caused by DNP additional addition. Figure 5 illustrates the thermogenic activity of tissue mitochondria in two states of metabolic activity. Oxygen uptake is correlated with the temperature increases in the transition from the resting to the active and to uncoupled states for mitochondria as measured by Estabrook and Poe using differential calorimetry. The calorimetric data of Estabrook and Poe in Fig. 5 show both respiratory activation and two fold increase in heat generation in mitochondrial [State 3, ADP activation] and a further two fold increase in the uncoupled State 3 [or State 6] in which the heat generation increases from 0.302 to 0.604 cal/min.

The NIR signals are measured with respect to a reference signal as has been necessary in the studies of the cytochromes of mitochondria by Chance and Williams.^{15–20}

4. The Future of Translational Optical Devices for Breast Cancer Detection

The difficult task of tracking and processing multiple biological signals {Biomarkers} from animal and human tissues is of increasing importance as the signal-rich Near Infra Red region should be in more detail. Here we have selected the intrinsic three Biomarkers of importance in the early detection of Human cancer that has been successfully used in the spectroscopic identification of the pigments of tissue mitochondria. We have not implemented any extrinsic Biomarkers that have been used in animal studies mainly due to clearing safety issues. The NIR technology is ready for detecting any novel biomarkers.

The great advantages of unfettered monitoring, data bank storage and multidimensional display moves medicine one step forward toward higher economy, higher throughput and most important, move early cancer signaling to the personalized home care.

A novel paradigm for breast cancer detection solves the difficult four multi-source — detector probe by miniaturized, handheld scanners which are small enough to be rapidly scanned over the breast, to give alert warning signals when an above threshold subsurface anomaly is detected, to give vector location and signal magnitude due display and at the signal crossover point to report the three biomarker signals for up to 8 detectors for entry in to a 3D data bank for evaluation by the radiologist for triage to the further detection devices.

References

1. L. Adrian, "Sir Charles Scott Sherrington O.M., 1857–1952," *Notes and Records of the Royal Society of London* **12**, 211–215 (1957).
2. A. Beckman, <http://www.beckman-foundation.com/founder.html>.
3. R. W. Burns, Russell W., *The Life and Times of A. D. Blumlein* (IEEE History of Technology series, 2000).
4. http://www.ieee.org/web/aboutus/history_center/biography/rajchman.html.
5. Britton Chance Patent US Patents: 2228199, 2228200, 2102511, 2102512, 2102513, 2132676, 2132677, 2182696, 2182717, 2185074, 2289242, 2337589.
6. K. L. Wildes and N. A. Lindgren, *A Century of Electrical Engineering and Computer Science at MIT, 1882–1982* (K. L. Wildes, Nilo. A. Lindgren, MIT Press 1985).
7. J. Stokes, *70 Years of Radio Tubes and Valves* (Vestal Press, NY, 1982), pp. 111–115.
8. J. W. Perry, "The F/1.8 quartz monochromator-spectrograph," *Trans. Opt. Soc.* **33**, 159–175 (1931).
9. H. A. Krebs, *Otto Warburg: Cell Physiologist, Biochemist and Eccentric* (Oxford University Press 1981).
10. B. Chance, "Rapid and sensitive spectrophotometry. I. The accelerated and stopped-flow methods for the measurement of the reaction kinetics and spectra of unstable compounds in the visible region of the spectrum," *Rev. Sci. Instru.* **22**, 619–627 (1951).
11. E. C. Slater, "Reflections Keilin, cytochrome and the respiratory chain," *J. Biol. Chem.* **278**, 16455–16461 (2003).
12. B. Chance, "The kinetics of the enzyme-substrate compound of peroxidase," *J. Biol. Chem.* **151**, 553–577 (1943).
13. A. Claude, "Electron microscope studies of cells by the method of replicas," *J. Exp. Med.* **89**, 425 (1949).
14. B. Chance, "Rapid and sensitive spectrophotometry. III. A double beam apparatus," *Rev. Sci. Instru.* **22**, 634–638 (1951).
15. B. Chance and G. R. Williams, "Respiratory enzymes in oxidative phosphorylation. I. Kinetics of oxygen utilization," *J. Biol. Chem.* **217**, 383–393 (1955).
16. B. Chance and G. R. Williams, "Respiratory enzymes in oxidative phosphorylation. II. Difference spectra," *J. Biol. Chem.* **217**, 395–407 (1955).
17. B. Chance and G. R. Williams, "Respiratory enzymes in oxidative phosphorylation. III The steady state," *J. Biol. Chem.* **217**, 409–427 (1955).
18. B. Chance and G. R. Williams, "Respiratory enzymes in oxidative phosphorylation. IV The respiratory chain," *J. Biol. Chem.* **217**, 429–438 (1955).
19. B. Chance, G. R. Williams, W. F. Holmes and J. Higgins, "Respiratory enzymes in oxidative phosphorylation. V. A mechanism for oxidative phosphorylation," *J. Biol. Chem.* **217**, 439–451 (1955).
20. B. Chance and G. R. Williams, "A simple and rapid assay of oxidative phosphorylation," *Nature* **175**, 1120–1124 (1955).
21. B. Chance and G. R. Williams, "A method for the localization of sites for oxidative phosphorylation," **176**, 250–254 (1955).
22. F. F. Jöbsis, "Non-invasive infrared monitoring of cerebral and myocardial oxygen sufficiency and circulatory parameters," *Science* **198**, 1264–1267 (1977).
23. B. Chance, J. S. Leigh, H. Miyake, D. S. Smith, S. Nioka, R. Greenfeld, M. Finander, K. Kaufmann, W. Levy, M. Young, P. Cohen, H. Yoshioka and R. Boretsky, "Comparison of time resolved and unresolved measurements of deoxyhemoglobin in brain," *Proc. Natl. Acad. Sci. USA* **85**, 4971–4975 (1988).

24. M. S. Patterson, B. Chance and B. C. Wilson, "Time resolved reflectance and transmittance for the noninvasive measurement of tissue optical properties," *J. Appl. Optics* **28**, 2331–2336 (1989).
25. A. G. Yodh and B. Chance, "Spectroscopy and imaging with diffusing light," *Physics Today* **48**, 34–40 (1995).
26. J. C. Hebden and D. T. Delpy, "Enhanced time-resolved imaging with a diffusion model of photon transport," *Optics Letters* **19**, 311–313 (1994).
27. S. Fantini, M. A. Franceschini and E. Gratton, "Effective source term in the diffusion equation for photon transport in turbid media," *Appl Opt.* **36**, 156–163 (1997).
28. J. C. Hebden, A. Gibson, R. Yusof, N. Everdell, E. M. C. Hillman, D. T. Delpy, S. R. Arridge, T. Austin, J. Meek and J. S. Wyatt, "Three-dimensional optical tomography of the premature infant brain," *Phy. Med. Biol.* **47**, 4155–4166 (2002).
29. D. K. Joseph, T. J. Huppert, M. A. Franceschini and D. A. Boas, "Diffuse optical tomography system to image brain activation with improved spatial resolution and validation with functional magnetic resonance imaging," *Applied Optics* **45**, 8142–8151 (2006).
30. H. Koizumi, T. Yamamoto, A. Maki, Y. Yamashita, H. Sato, H. Kawaguchi and N. Ichikawa, "Optical topography: practical problems and new applications," *Appl. Opt.* **42**, 3054–3062 (2003).
31. D. Grosenick, H. Wabnitz, K. T. Moesta, J. Mucke, M. Möller, C. Stroszczynski, J. Stössel, B. Wassermann, P. M. Schlag and H. Rinneberg, "Concentration and oxygen saturation of haemoglobin of 50 breast tumours determined by time-domain optical mammography," *Phys. Med. Biol.* **49**, 1165–1181 (2004).
32. T. D. Yates, J. C. Hebden, A. P. Gibson, N. L. Everdell, D. T. Delpy, S. R. Arridge, M. Douek and W. Chicken, "Clinical results from a 32-channel time resolved system used to image the breast," *OSA Biomedical Topical Meetings*, Miami WF18 (2004).
33. P. Taroni, G. Danesini, A. Torricelli, A. Pifferi, L. Spinelli and R. Cubeddu, "Clinical trial of time-resolved scanning optical mammography at 4 wavelengths between 683 and 975 nm," *J. Biomed. Opt.* **9**, 464–473 (2004).
34. B. Chance, M. T. Dait, C. Zhang, T. Hamaoka and F. Hagerman, "Recovery from exercise-induced desaturation in the quadriceps muscles of elite competitive rowers," *Am. J. Physiol.* **262**, C766–C775 (1993).
35. J. Im, D. Nioka, B. Chance and K. W. Rundell, "Muscle oxygen desaturation is related to whole body VO₂ during cross-country ski skating," *Int. J. Sports Med.* **22**, 356–360 (2001).
36. L. Szmedra, J. Im, S. Nioka, B. Chance and K. Rundell, "Hemoglobin/myoglobin oxygen desaturation during Alpine skiing," *Med. Sci. Sports Exerc.* **33**, 232–236 (2001).
37. <http://www.nellcor.com/prod/List.aspx?S1=POX>.
38. G. A. Millikan, J. R. Pappenheimer, A. J. Rawson *et al.*, "The continuous measurement of arterial saturation in man," *Am. J. Physiol.* **133**, 390 (1941).
39. G. Gratton, C. R. Brumback, B. A. Gordon, M. A. Pearson, K. A. Low and M. Fabiani, "Effects of measurement method, wavelength and source," *Neuroimage.* **32**, 1576–1590 (2006).
40. S. Ogawa, R. S. Menon, D. W. Tank, S. G. Kim, H. Merkle, J. M. Ellermann and K. Ugurbil, "Functional brain mapping by blood oxygenation level-dependent contrast magnetic resonance imaging. A comparison of signal characteristics with a biophysical model," *Biophys. J.* **64**, 803–812 (1993).
41. B. Chance, S. Nioka, S. Sadi and C. Li, "Oxygenation and blood concentration changes in human subject prefrontal activation by anagram solutions," *Adv. Exp. Med. Biol.* **510**, 397–401 (2003).

42. M. Izzetoglu, K. Izzetoglu, S. Bunce, A. Ayaz, A. Devarai, B. Onaral and K. Pourrezaei, "Functional near-infrared neuroimag in neural systems and rehabilitation engineering," *IEEE Transactions* **13**, 153–159 (2005).
43. <http://www.infrascanner.com/>.
44. B. Chance, S. Nioka, J. Zhang, E. F. Conant, E. Hwang, S. Briest, S. G. Orel, M. D. Schnall and B. J. Czerniecki, "Breast cancer detection based on incremental biochemical and physiological properties of breast cancers: A six year, two site study," *Acad. Radiol.* **12**, 925–33 (2005).
45. B. Chance, K. Kang, L. He, H. Liu and S. Zhou, "Precision localization of hidden absorbers in body tissues with phased-array optical systems," *Rev. Sci. Instru.* **67**, 4324–4332 (1996).
46. J. M. Schmitt, A. Knuttel *et al.*, "Interference of diffusive light waves," *J. Opt. Soc. Am.* **9**, 1832 (1992).
47. A. Knuttel, R. Barnes and J. R. Knutson, "Acousto-optic scanning and interfering photon density waves for precise localization of an absorbing (or fluorescent) body in a turbid medium," *Rev. Sci. Instrum* **32**, 381–389 (1993).
48. J. J. Kelly, K. A. Kelly, C. H. Barlow and C. H. Ed, "Tissue temperature by near-infrared spectroscopy. Optical tomography, photon migration and spectroscopy of tissue and model media," *SPIE* **2389**, 818–828 (1995).
49. M. Poe and R. W. Estabrook, "Kinetic studies of temperature changes and oxygen uptake in a differential calorimeter: The heat of oxidation of NADH and succinate," *Arch. Biochem. Biophys.* **122**, 204–211 (1967).